

Fe-bump instability: the excitation of pulsations in subdwarf B and other low-mass stars

C.S. Jeffery^{*} & H. Saio[†]

Armagh Observatory, College Hill, Armagh BT61 9DG, Northern Ireland

Astronomical Institute, School of Science, Tohoku University, Sendai 980-8578, Japan

Accepted Received ; in original form

ABSTRACT

We consider the excitation of radial and non-radial oscillations in low-mass B stars by the iron-bump opacity mechanism. The results are significant for the interpretation of pulsations in subdwarf B stars, helium-rich subdwarfs and extreme helium stars, including the EC14026 and PG1716 variables.

We demonstrate that, for radial oscillations, the driving mechanism becomes effective by increasing the contrast between the iron-bump opacity and the opacity from other sources. This can be achieved either by increasing the iron abundance or by decreasing the hydrogen abundance. The location of the iron-bump instability boundary is found to depend on the mean molecular weight in the envelope and also on the radial order of the oscillation. A bluer instability boundary is provided by increasing the iron abundance alone, rather than the entire metal component, and is required to explain the observed EC14026 variables. A bluer instability boundary is also provided by higher radial order oscillations. Using data for observed and theoretical period ranges, we show that the coolest EC14026 variables may vary in the fundamental radial mode, but the hottest variables *must* vary in modes of higher radial order.

In considering non-radial oscillations, we demonstrate that g-modes of high radial order and low spherical degree ($l < 4$) may be excited in some blue horizontal branch stars with near-normal composition ($Z = 0.02$). Additional iron enhancement extends the g-mode instability zone to higher effective temperatures and also creates a p-mode instability zone. The latter is essentially contiguous with the radial instability zone. With sufficient iron, the p-mode and g-mode instability zones overlap, allowing a small region where the EC14026 and PG1716-type variability can be excited simultaneously. The overlap zone is principally a function of effective temperature and only weakly a function of luminosity. However its location is roughly 5000K too low compared with the observed boundary between EC14026 and PG1716 variables. The discrepancy cannot be resolved by simply increasing the iron abundance.

Key words: stars: oscillations, stars: subdwarfs, stars: horizontal branch, stars: chemically peculiar, stars: early-type, stars: variables: other

1 INTRODUCTION

The discovery of a significant contribution to stellar opacity from iron-group elements at temperatures around 200 000 K (Rogers & Iglesias 1992; The Opacity Project Team 1995) had major consequences for studies of pulsation in stars. First, it solved the long-standing Cepheid mass problem (Moskalik, Buchler & Marom 1992; Kanbur & Simon 1994). Second, it provided a natural explanation for hitherto un-

explained stellar variability, notably with respect to the β Cepheids (Dziembowski & Pamiatnykh 1993) and some extreme helium stars (Saio 1993). Third, it initiated searches for variability (predicted and observed) in stars hitherto thought to be stable. There are now known to be several classes of variable in which pulsations are driven by the opacity (or κ -) mechanism excited by the Fe- or Z- opacity bump. It is one goal of this paper to explore some of the connections between these groups and hence to understand better the nature of Fe-bump driven pulsations.

An early success was the explanation of radial pulsations in the extreme helium star V652 Her (Saio 1993), to-

^{*} E-mail: csj@arm.ac.uk

[†] E-mail: saio@astr.tohoku.ac.jp

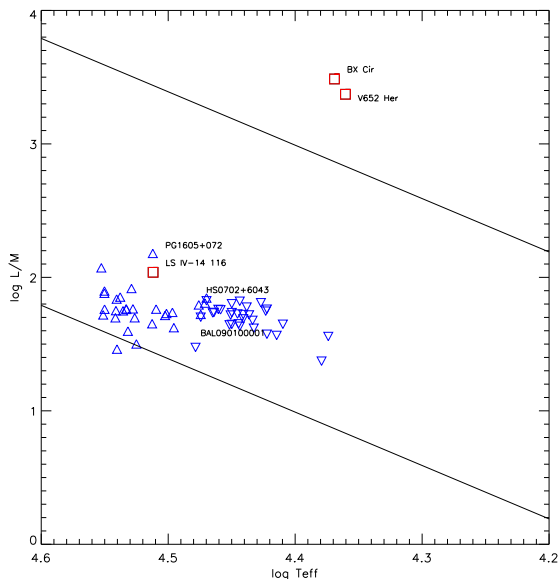


Figure 1. The loci of low-mass variable stars believed to pulsate due to Fe-bump instability, including EC14026 variables (upright triangles), PG1716 variables (inverted triangles) and helium-rich variables (squares). A selection are labeled. HS0702+6843 and Balloon 090100001 exhibit both EC14026 and PG1716-type behaviour (Schuh et al. 2006; Oreiro et al. 2005). Straight diagonal lines represent $\log g = 6.0$ (below) and 4.0 (above). These features are reproduced in Figs. 2 to 5.

gether with the prediction (Saio 1994) and subsequent discovery of radial pulsations in a second helium star, BX Cir (Kilkenny & Koen 1995). In these stars, both with periods of ~ 9300 s and with masses 0.59 and $0.47 M_{\odot}$ respectively (Jeffery, Woolf & Pollacco 2001; Woolf & Jeffery 2002) (Fig. 1), the cause of pulsation instability is clearly the Fe- opacity bump, exaggerated by a reduction of the background opacity due to hydrogen at these temperatures. The failure to detect any variability in a third helium star, HD144941, of similar temperature and luminosity but very low metallicity (Jeffery & Hill 1996; Jeffery & Harrison 1997), confirmed the rôle of the Fe-opacity in driving pulsations in these low-mass early-type stars.

Another notable success has been the prediction and discovery of short-period pulsations in subluminescent B (sdB) stars (Charpinet et al. 1996, 1997; Kilkenny et al. 1997; Billères et al. 1997). Briefly, multi-periodic oscillations with periods between 90 and 600 seconds are observed in approximately 10% of hot subdwarf B stars; such stars are variously known as EC14026 variables (after the class prototype EC 14026–2647) or sdBVs. These pulsations are successfully explained if the stars are “extreme horizontal branch stars”, that is they consist of a helium-burning core of some $0.5 M_{\odot}$ overlaid by a very thin layer of hydrogen. Because of the high effective temperature and the high surface gravity, theoretical models have shown that radiative forces on the ions in the stellar envelope act differentially such that substantial chemical gradients are established over a diffusion time scale $\sim 10^5$ y (Michaud et al. 1989). The consequent levitation and accumulation of iron in layers at around 200 000 K (Chayer, Fontaine & Wesemael 1995) en-

hances the Fe-opacity bump sufficiently that radial and non-radial p-mode oscillations are excited. The theory successfully explained the observed distribution (Fig. 1) of pulsating and non-pulsating sdB stars in effective temperature and surface gravity (Charpinet et al. 2001). Although consequential more on frequency eigenvalues than stability criteria, the theory is also sufficiently well developed that it has been possible to compare predicted and observed pulsation frequencies in some pulsating sdB stars (Brassard et al. 2001; Charpinet et al. 2005a,b).

The unexpected discovery of oscillations with periods of a few hours in many sdB stars lying red-ward of the EC14026 instability domain presented a new challenge (Green et al. 2003). While radiative levitation of iron is still operative in these stars, sometimes known as PG1716 variables (after the prototype PG 1716+426), p-modes are reported to be stable in the chemically stratified models (Charpinet et al. 2001). On the other hand, non-radial g-modes of high radial order ($k \geq 10$) and high spherical degree ($l \geq 3$) were found to be unstable, but only in models of stars cooler than those in which variability had been detected (Fontaine et al. 2003). While the observed periods imply a g-mode origin, modes of such high degree are not generally thought to be observable as variations in total flux due to geometric cancellation. The challenge is therefore to shift the g-mode blue edge to higher effective temperatures and to excite modes of lower spherical degree.

A further challenge has been provided by the detection of variability in the helium-rich sdB star LS IV–14°116 with periods of $\sim 1800 - 3000$ s (Ahmad & Jeffery 2005). While the canonical sdB stars mostly have surface helium abundances one tenth of the solar value ($\sim 10\%$ by number), the much rarer He-rich sdB stars comprise a spectroscopically distinct and highly inhomogeneous group with surface helium abundances ranging from some 30% to nearly 100% by number, and surface gravities over a much broader range than seen in normal sdB stars (Ahmad & Jeffery 2003). The natural response to the discovery of pulsations in LS IV–14°116 was to try to explain them in terms of Fe-bump instability in either a helium star like V652 Her, or in some sort of mutant sdB star. With T_{eff} similar to the EC14026 stars, but with a lower surface gravity (higher L/M ratio), the pulsation periods were too long to be explained by Fe-bump driven p-modes (Ahmad & Jeffery 2005). One question is whether g-modes might be excited in such a star. This challenge is important because a viable picture of the star that explains both the L/M ratio and the high surface abundance of helium has yet to be established. Any model that successfully reproduced the observed oscillations would assist this process.

In order to address these questions, we need to develop our understanding of instability in low-mass stars. By gaining a general insight into what affects the type of pulsation that can be driven, it should be possible to determine what model properties need to be modified in order to reproduce observed oscillations.

The important theme is clearly Fe-bump instability. We have already investigated the rôle of envelope hydrogen abundance in the excitation of Fe-bump pulsations (Jeffery & Saio 1998). We recall that pulsational instability exists in all stars of sufficiently high L/M ratio due to the presence of strange-mode instability (Gautschi & Glatzel

1990). Fe-bump instability sets in for lower L/M stars with $T_{\text{eff}} \sim 20 - 30\,000\text{K}$ when either the iron-abundance is raised sufficiently or the hydrogen abundance is reduced sufficiently. The second occurs because reducing the hydrogen opacity increases the contrast between the iron opacity and the background opacity due to other sources, effectively increasing the opacity gradients $\kappa_T = (\partial \ln \kappa / \partial \ln T)_\rho$, $\kappa_\rho = (\partial \ln \kappa / \partial \ln \rho)_T$ in the driving zone.

Therefore there should be a physical connection between, for example, the radial pulsations seen in the extreme helium star V652 Her (essentially normal iron, reduced hydrogen) and the p-mode oscillations in EC14026 variables (normal hydrogen, enhanced iron). Note that radial modes are special cases of p-modes with spherical degree $l = 0$; such modes are generally present in EC14026 stars alongside modes of higher spherical degree. However, the EC14026 instability region reported by Charpinet et al. (2001) lies considerably blue-ward of the Fe-bump instability finger described by Jeffery & Saio (1998). Understanding this paradox represents an important step towards understanding Fe-bump instability in general.

Our initial goal is therefore to explore Fe-bump instability for radial modes in comparatively simple (i.e. homogeneous) stellar envelopes as a function of composition (section II). With success here, it becomes possible to restrict the volume of model space required to explore the stability of modes of higher degree, in particular g-modes (section III), and also to identify what is required in more detailed models in order to reproduce the observations accurately.

2 RADIAL MODES

Linear non-adiabatic models of radial pulsations have been constructed following the method described by Saio (1995), but including the most recent OPAL95 opacities (Iglesias & Rogers 1996). In all cases the equation of state (EOS) treats hydrogen, helium and a representative “metal”, namely carbon. The contribution to the EOS of varying the heavy element distribution within “Z” is negligible at temperatures above 10 000 K since both the electron density and the mean atomic weight are completely dominated by hydrogen and helium.

The parameter range considered is $M/M_\odot = 0.4 - 0.9$, $\log T_{\text{eff}}/K = 4.20 - 4.60$ and $\log L/M = 0.4 - 3.8$ (solar units). In terms of composition, the hydrogen mass fraction $X = 0.0 - 0.9$ includes extremely helium-rich, normal and helium-depleted mixtures. The treatment of metal mass fraction Z is discussed below. The choice of L/M rather than L as independent variable was made because pulsation properties scale roughly with M (actually $M^{1/2}$), simplifying the generation of model grids and the inter-comparison of results for different masses.

For each combination of M , T_{eff} , L/M , X and Z , a homogeneous static stellar envelope is integrated assuming a standard surface boundary condition. This integration is terminated when the total pressure exceeds 10^{17} dyn or the mass variable $< 0.6M$, whichever occurs first. This limit is justified for a stability analysis of radial modes (and p-modes in general) since amplitudes decay exponentially towards the stellar center. However, the accurate prediction of

periods for asteroseismology (for example) must use whole-star models so as to account for higher order effects.

The first several eigenfrequencies are located and stored, including the real and imaginary components ω_r and ω_i , the period Π and the number of nodes in the eigensolution. So far, it has not been necessary to analyze more than the first ten eigenfrequencies; the maximum number of unstable modes located so far was nine. The results have been collated as diagrams showing the stability of one or more modes and the number of unstable modes as a function of T_{eff} and L/M . Stability is established by the sign of ω_i (negative for unstable modes). Results for varying X and Z are compared in a mosaic of similar such diagrams, on which are superposed the loci of selected groups of variable star.

When identifying eigenfrequencies it is usual to identify the fundamental, first overtone, second overtone, etc, in sequence for each model envelope, as verified by the number of nodes in the eigensolution. However, in the most luminous models, strange mode pulsations are excited and the one-to-one correspondence between the ordinal number of the eigensolution identified and the number of its radial nodes frequently breaks down. The physics of this question are discussed in more detail elsewhere (Saio, Baker & Gautschy 1998); it has no effect on the results presented here.

Z variation

The first experiment was carried out on the basis that increasing the overall metallicity is known to increase the size of the Fe-bump instability. Calculations were carried out for $Z = 0.01, 0.02, 0.05, 0.10$ and 0.20 . X was reduced to 0.80 when $X + Z > 1$ would otherwise have resulted. This is essentially a repeat of the experiment described by Charpinet et al. (2001) but over a much larger volume of parameter space.

Figures 2 and 3 show how the resulting instability boundaries behave as functions of X and Z for a mass of $0.50 M_\odot$. The results for other masses ($0.4, 0.7$ and $0.9 M_\odot$) are similar. The discrete model grid is reflected in the contour shapes. Note that all the panels have hydrogen abundance increasing from bottom to top and metallicity (in whatever form) increasing from left to right.

For clarity, Fig. 2 shows the instability boundaries for only the radial fundamental and the first, second and third radial overtones ($k = 0, 1, 2, 3$). It demonstrates a number of important general features.

- 1) The Fe-bump instability finger is not significant for normal abundances ($X = 0.75, Z = 0.02$).
- 2) The size of the instability finger increases with increasing Z and with decreasing X .
- 3) For increasing Z , the number of excited nodes increases.
- 4) The Fe-bump instability region, including the blue edge, becomes bluer for higher order modes (a similar result holds for the classical HeII instability strip).
- 5) The blue edge for any given mode (e.g. the fundamental) is not shifted significantly by increasing Z , while the red edge is shifted red-ward.
- 6) The low-luminosity end of the instability finger is populated by the highest number of excited modes.
- 7) Unstable modes with $L/M \geq 3.5$ are primarily strange modes.

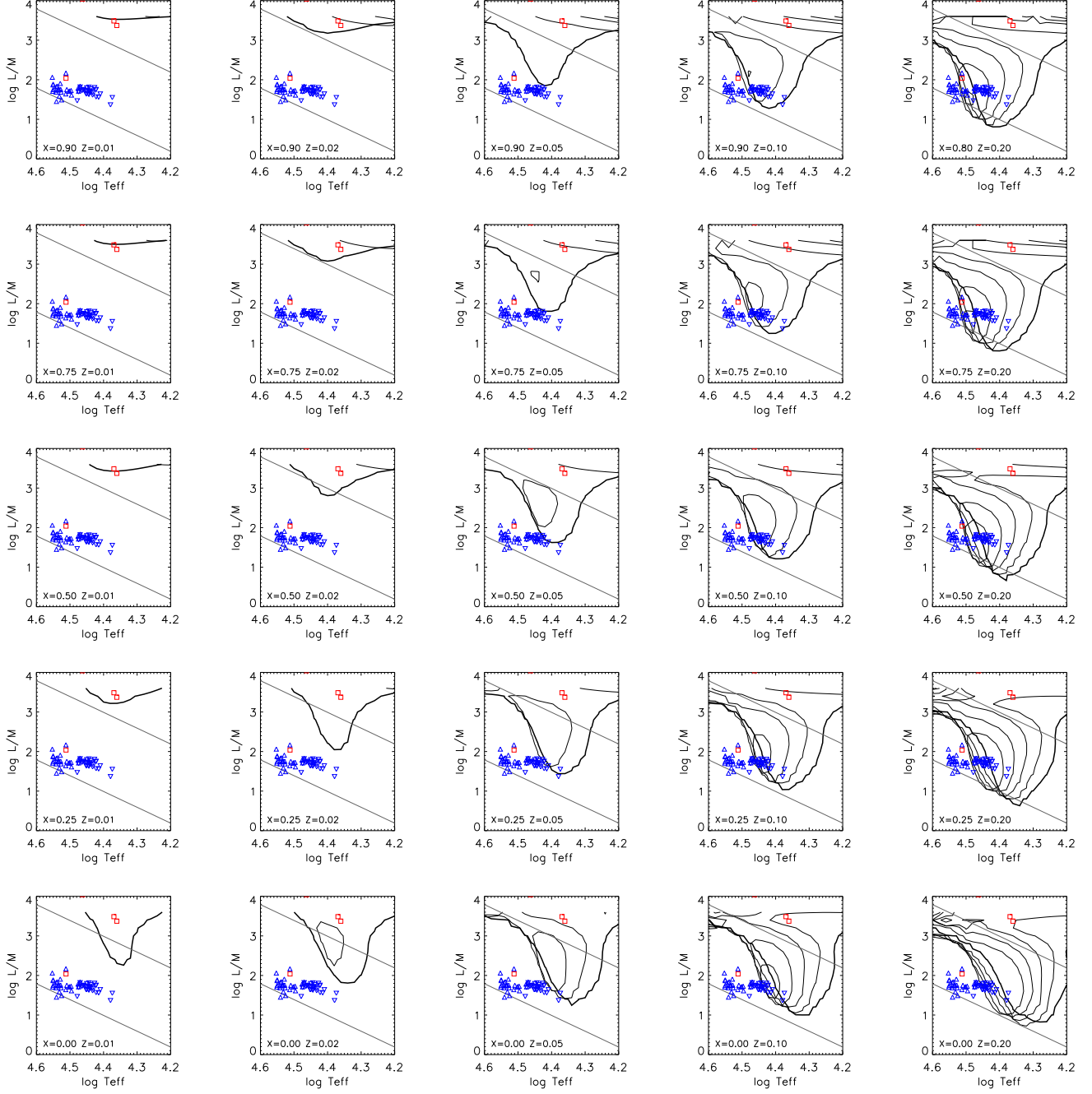


Figure 2. Instability boundaries for radial pulsation modes in stars with $M = 0.5 M_{\odot}$ and homogeneous envelopes with $Z = 0.01 - 0.20$. The bold line shows the instability boundary for the longest period radial mode, normally the fundamental $k = 0$. Thin contours show successive boundaries for $k = 1, 2, 3$, where these exist. Other features as in Fig. 1.

Figure 3 presents an alternative view of the same results but, because it includes all the excited modes up to $k = 10$, it reflects the extent and mode-density of the instability region more effectively. Many of these features were already well known from previous studies (Jeffery & Saio 1998; Charpinet et al. 2001), but it is helpful to reiterate them here in one unified picture.

In terms of matching the observations of the EC14026 stars and objects like LSIV-14°116, this figure shows that

at these high T_{eff} , radial modes (and hence p-modes in general) are not excited, even for very high Z (cf. Fig. 3 in Charpinet et al. 2001). Despite the excitation of higher-order modes with slightly bluer blue edges, the extension to the instability zone is insufficient.

This has a natural explanation. In attempting to shift the instability boundary, Z has been increased in order to increase the driving by the Fe-opacity bump. At the same time the mean molecular weight of the gas and the mean

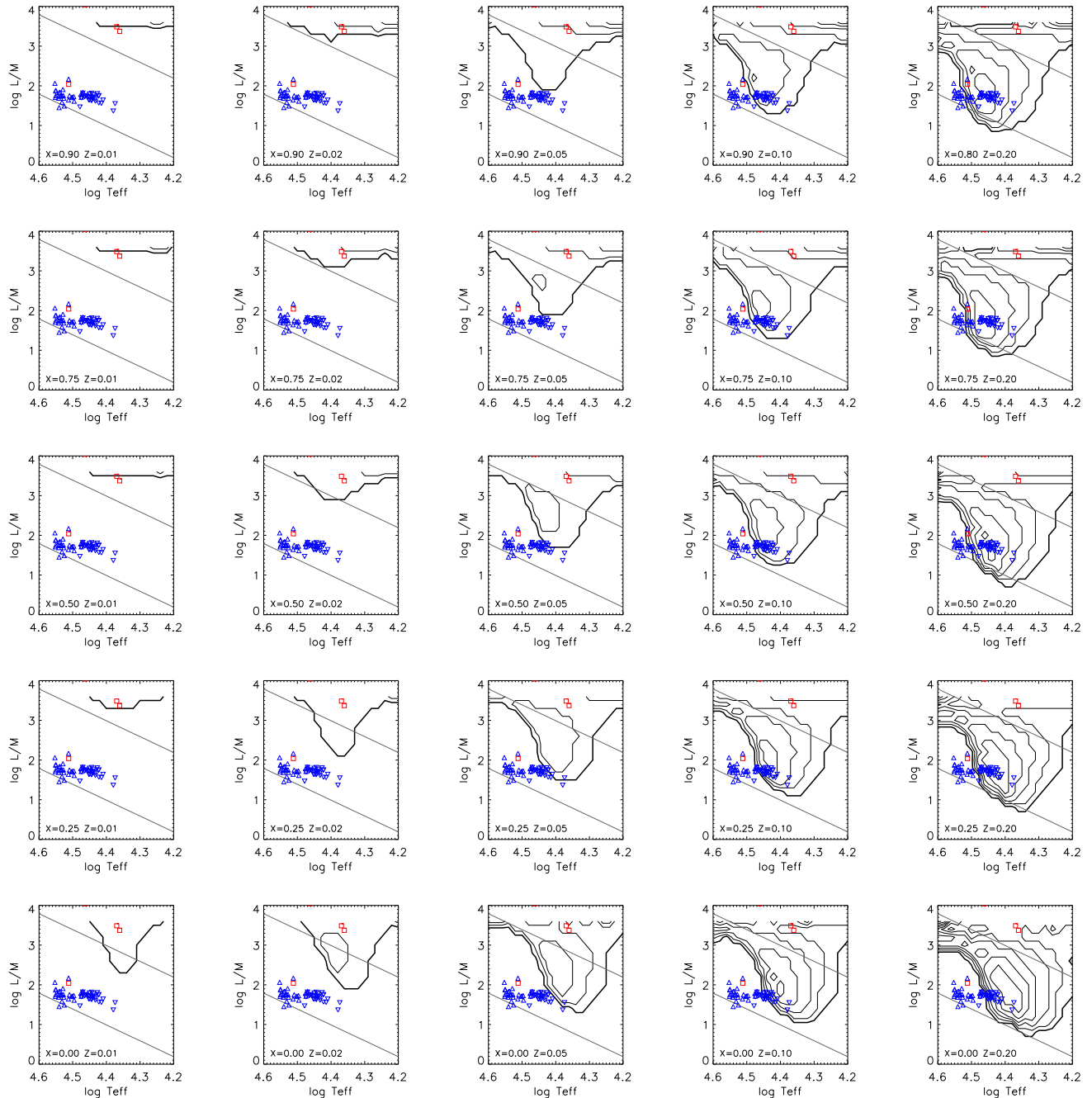


Figure 3. The number of unstable radial pulsation modes in stars with $M = 0.5 M_{\odot}$ and homogeneous envelopes with $X = 0.0 - 0.9$ and $Z = 0.01 - 0.20$. The bold line shows the overall instability boundary; within this contour at least one radial mode is excited. Each subsequent contour (thin lines) represents one additional unstable mode. Other features as in Fig. 1.

opacity in the layers above the driving zone has been increased. Therefore the Fe-bump will be located correspondingly closer to the stellar surface. In order to make the blue edge bluer, it is necessary to maintain the contribution to driving from iron without increasing the mean molecular weight and opacity in the layers above the driving layer.

Fe variation

The logical alternative is therefore to increase the iron abundance *without* increasing the abundances of other heavy elements. Using the OPAL opacity table generator (Iglesias & Rogers 1996), we constructed new sets of opacity tables in which the iron abundance alone was increased by factors of $f = 5, 10$ and 20 , whilst the remaining elements had abundances corresponding to a $Z = 0.02$ mixture. There is a modest effect on the overall Z such that

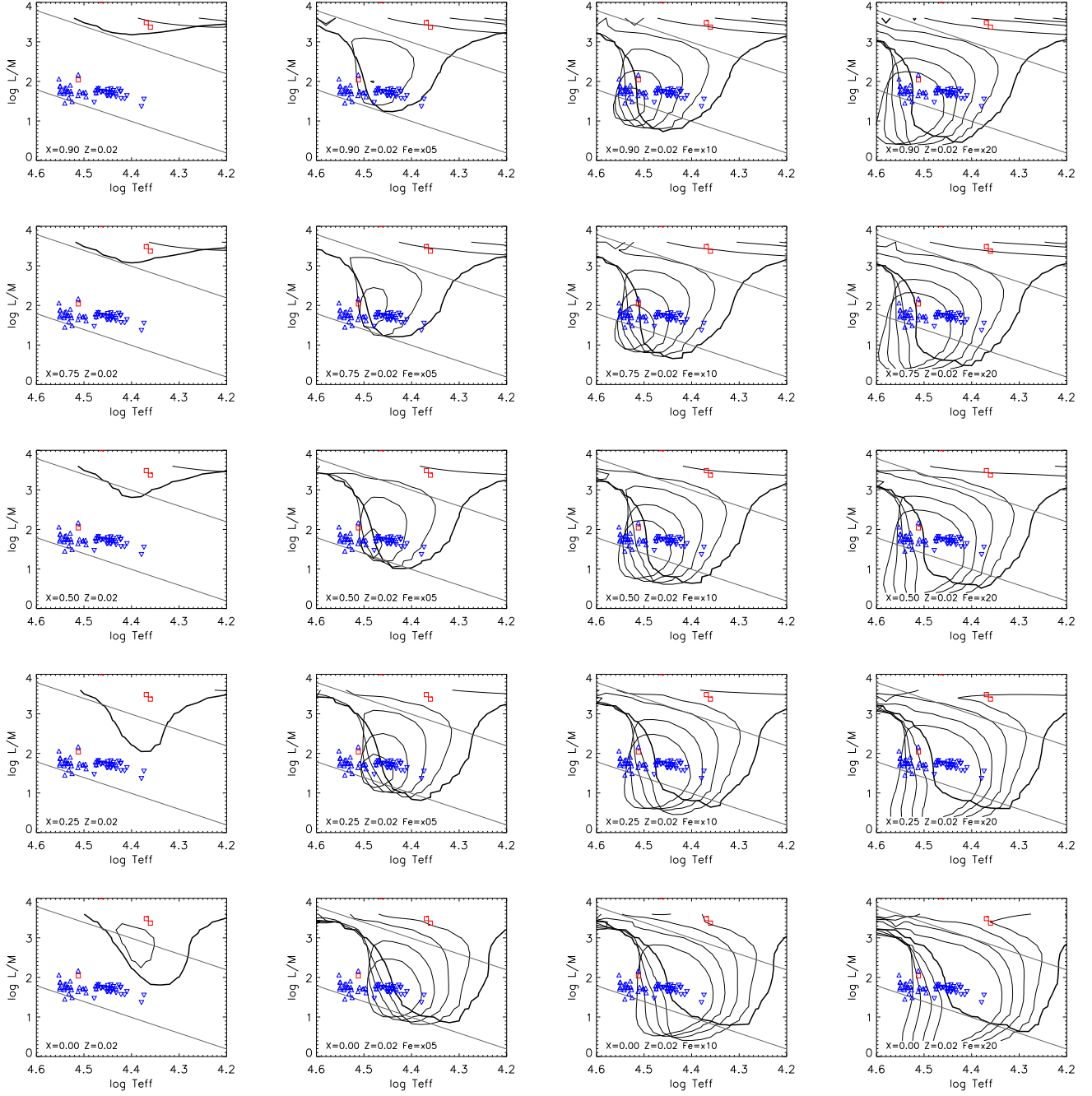


Figure 4. As Fig. 2 but with $Z = 0.02$ and Fe enhanced by factors of 1, 5, 10 and 20.

$Z = 0.02 + (f - 1)Z_{\text{Fe}}$ where $Z_{\text{Fe}} = 0.02188$ represents the mass fraction of iron within the standard heavy element mixture (Grevesse & Noels 1993). A similar set of models was run for these mixtures. These are compared with the reference set $Z = 0.02$ in Figs. 4 and 5.

It is immediately apparent that increasing the iron abundance alone by a factor five produces a predictable effect similar to increasing Z from 0.02 to 0.10, but with the major difference that the blue edge has become bluer and more vertical (in the $L/M - T_{\text{eff}}$ diagram). As the iron abundance is further increased (*cf.* $X = 0.75, Z = 0.02, f = 10$),

a region develops which contains several excited modes and which is bluer than the Fe-bump instability finger seen when the entire Z -component varies together.

This is precisely the phenomenon identified by Charpinet et al. (1997). The overall extent of our instability zone is larger than identified before; the earlier calculations benefit from obeying a total iron conservation law by using an iron distribution obtained from a self-consistent calculation of radiative levitation.

The significance here is that earlier results are reproduced in character, if not in detail, using a simple model. It

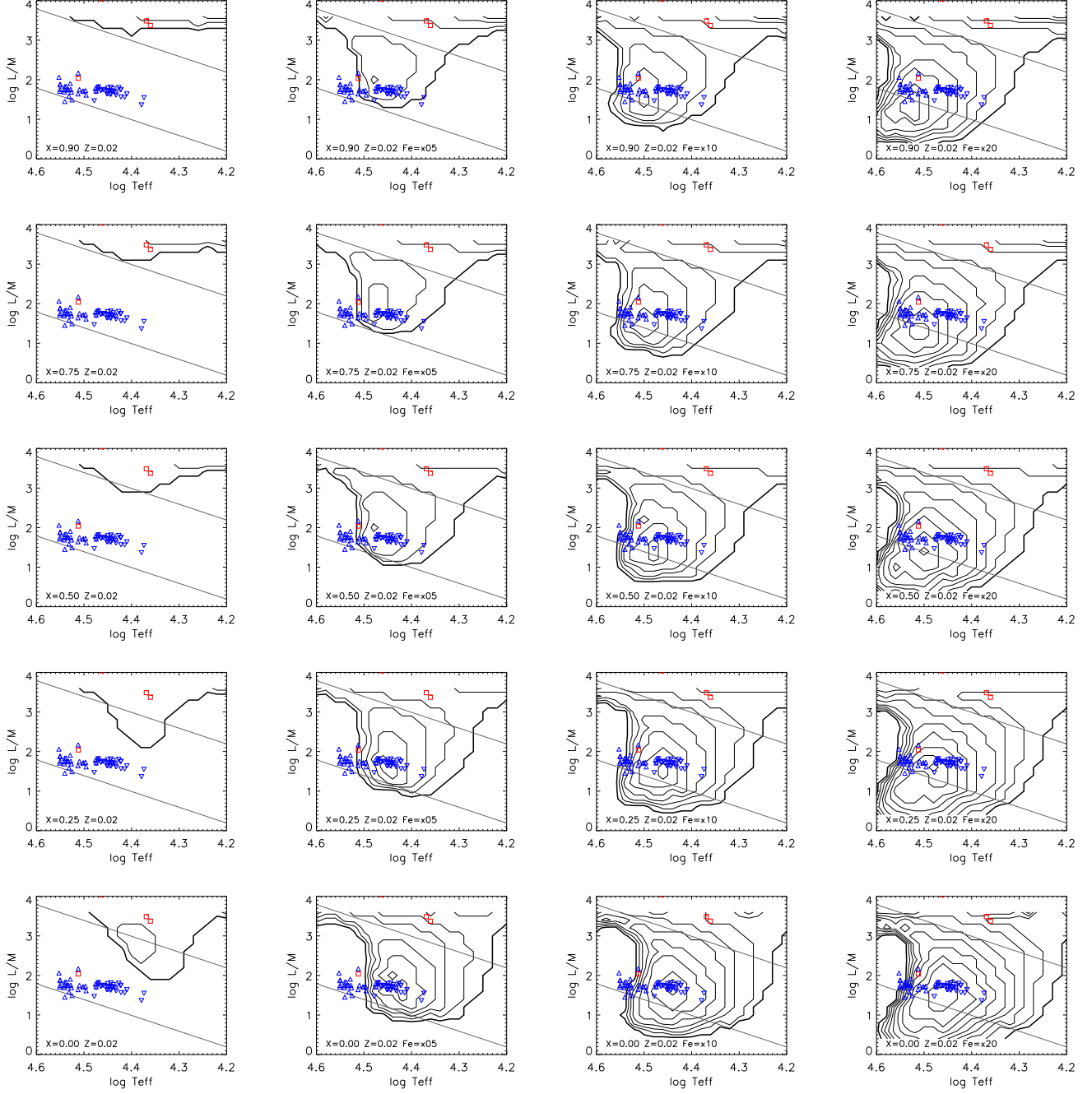


Figure 5. As Fig. 3 but with $Z = 0.02$ and Fe enhanced by factors of 1, 5, 10 and 20.

tells us that the principal characteristics of p-mode instability in EC14026 stars may be derived from a homogeneous stellar envelope with a factor 10 enhancement in iron abundance (assuming $Z \sim 0.02$). This provides useful pointers for a subsequent investigation of g-mode instability.

It is interesting that reducing hydrogen concentration extends the instability finger towards lower L/M and lower T_{eff} . Whether this region of parameter space is populated by any real stars is a matter for conjecture. If they do, they are likely helium- and iron-rich white dwarfs with periods of \sim seconds. However, diffusion theory suggests that in stars of

such high gravity, iron would settle out of the layers where it would be required to excite pulsations.

To understand the phenomenon we recall that the instability blue edge occurs when the thermal timescale

$$\tau_{\text{th}} = c_v T \Delta m / L \quad (1)$$

becomes too small compared with the pulsation period, where T is the temperature in the excitation layer, c_v is the specific heat per unit mass at constant volume, and Δm is the mass lying above the excitation layer (see Cox 1980, Ch. 10 for details). Let us assume an ideal gas and that the

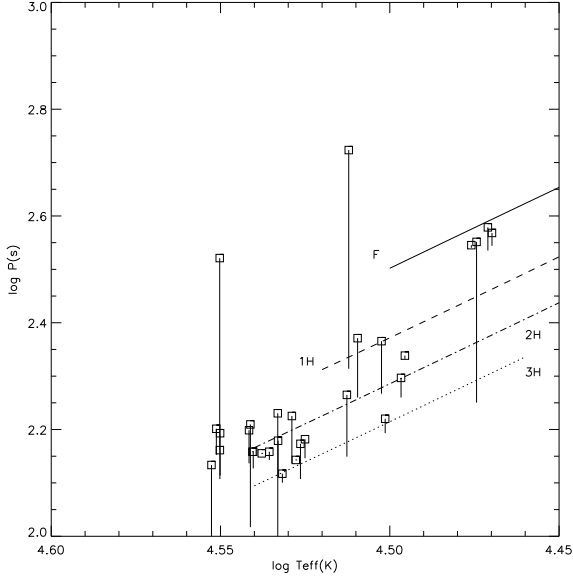


Figure 7. Fig. 6 redrawn with the observed periods of EC14026 stars over-plotted on the theoretical periods of unstable radial modes for $M = 0.50 M_{\odot}$, $\log L/M = 1.8$, $X = 0.75$, $Z = 0.02$ and enhanced iron ($f = 10$). The modes are labeled by radial degree.

opacity in the layers above the excitation zone is expressed as

$$\kappa = \kappa_0 \rho^a T^{-b} \quad (2)$$

with constants κ_0 , a ($0 \leq a \leq 1$), and b . Then, we can integrate approximately, from the stellar surface to the excitation zone, the hydrostatic equation and the equation of diffusive flow of radiation to obtain

$$\Delta m \propto (\kappa_0 L \mu^a M^a)^{-\frac{1}{1+a}} R^4, \quad (3)$$

where μ is the mean molecular weight and R is the stellar radius. Substituting equation (3) into equation (1), and taking into account $c_v \propto 1/\mu$, we have

$$\tau_{\text{th}} \propto (\kappa_0 \mu^{1+2a})^{-\frac{1}{1+a}} (L/M)^{\frac{a}{1+a}} T_{\text{eff}}^{-8}. \quad (4)$$

The strong dependence of τ_{th} on T_{eff} is responsible for the blue and the red edges of instability range. Since the κ -mechanism is optimal when the period of pulsation is comparable to τ_{th} , the instability range of a short (long) period mode is hotter (cooler) as can be seen in Figs. 2 and 4.

For a given L/M ratio, the blue-edge can be shifted blueward by increasing τ_{th} , *i.e.* by reducing κ_0 and the mean molecular weight μ . The former can be achieved by reducing Z without significantly reducing the iron abundance. The mean molecular weight is reduced by increasing X . The effect is somewhat complicated because an increase in X tends to increase κ_0 . Figs. 2 and 4 seem to indicate that the effect of reducing the mean molecular weight exceeds the effect of increasing opacity.

Periods

Predicted pulsation periods for unstable fundamental radial modes, and for first, second and third radial harmon-

ics are shown in Fig. 6 for a range of compositions and for $\log L/M = 1, 2$ and 3. The central column represents models with a standard metallicity and reduced hydrogen abundance, while the left and right columns represent a uniform metal enhancement and a selective iron enhancement respectively. Note again that the lower L/M pulsators for a selective iron enhancement are bluer than for a uniform enhancement, and also that higher-order modes are preferentially excited in bluer pulsators.

For comparison, the top centre panel shows the pulsation periods and period ranges for several EC14026 and extreme helium-star pulsators. A consequence of the models is that bluer EC14026 stars should show higher harmonics and, conversely, there should be fewer hot sdBVS pulsating in the radial fundamental mode. This is clearly reflected by the mean slope of the $\log P(\log T_{\text{eff}})$ relation for EC14026 stars (excluding PG 1605+072 and KPD 1930+2752) being steeper than that for a single mode. Fig. 7 compares the observations for EC14026 variables with pulsation periods for unstable radial modes with $M = 0.50 M_{\odot}$, $X = 0.75$, $Z = 0.02$ and enhanced iron ($f = 10$); $\log L/M = 1.8$ was chosen to be representative of the EC14026 variables (see Fig. 1). It is evident that only the coolest stars are likely to pulsate in the radial fundamental mode while many of the hottest can only excite the second or third harmonic. Some EC14026 stars lie beyond the blue-edge for all of these models; a higher value of f might have been more appropriate, but the overall result is unaffected.

Two exceptions are PG 1605+072 and KPD 1930+2752. The first has evolved away from the extreme horizontal-branch and has a higher L/M ratio (Fig. 1). The second is tidally distorted by a very close binary companion (Billères et al. 2000) and our classical radial models may be inadequate.

Growth Rates

An indication of the overall instability is given in Fig. 8 where the exponential growth times are shown as contour plots for compositions representative of extreme helium and EC14026 variables. The growth times are represented by the dimensionless quantity $-\omega_r/\omega_i$. Divide by 2π to find the growth time in pulsation cycles, and then multiply by pulsation period P to obtain the physical growth time τ_g . Thus, for the EC14026 stars with $M = 0.50 M_{\odot}$ and $\log L/M \sim 1.7$, Fig. 6 indicates $\log P/s \sim 2$ and Fig. 8 indicates $\log(-\omega_r/\omega_i) \sim 4$, yielding $\log \tau_g/s \sim 5$. For the extreme helium stars, the same exercise also gives $\log \tau_g/s \sim 5$. With growth times \sim one day, these modes are highly unstable.

3 NON-RADIAL MODES

Zero-age extreme horizontal-branch stars

The non-radial modes most usually observed in stars may be divided into pressure or p-modes and gravity or g-modes. Pressure modes are trapped in the outer stellar envelope and may be thought of as a three dimensional generalization of the radial modes discussed in the previous section. Therefore their stability has essentially been discussed already,

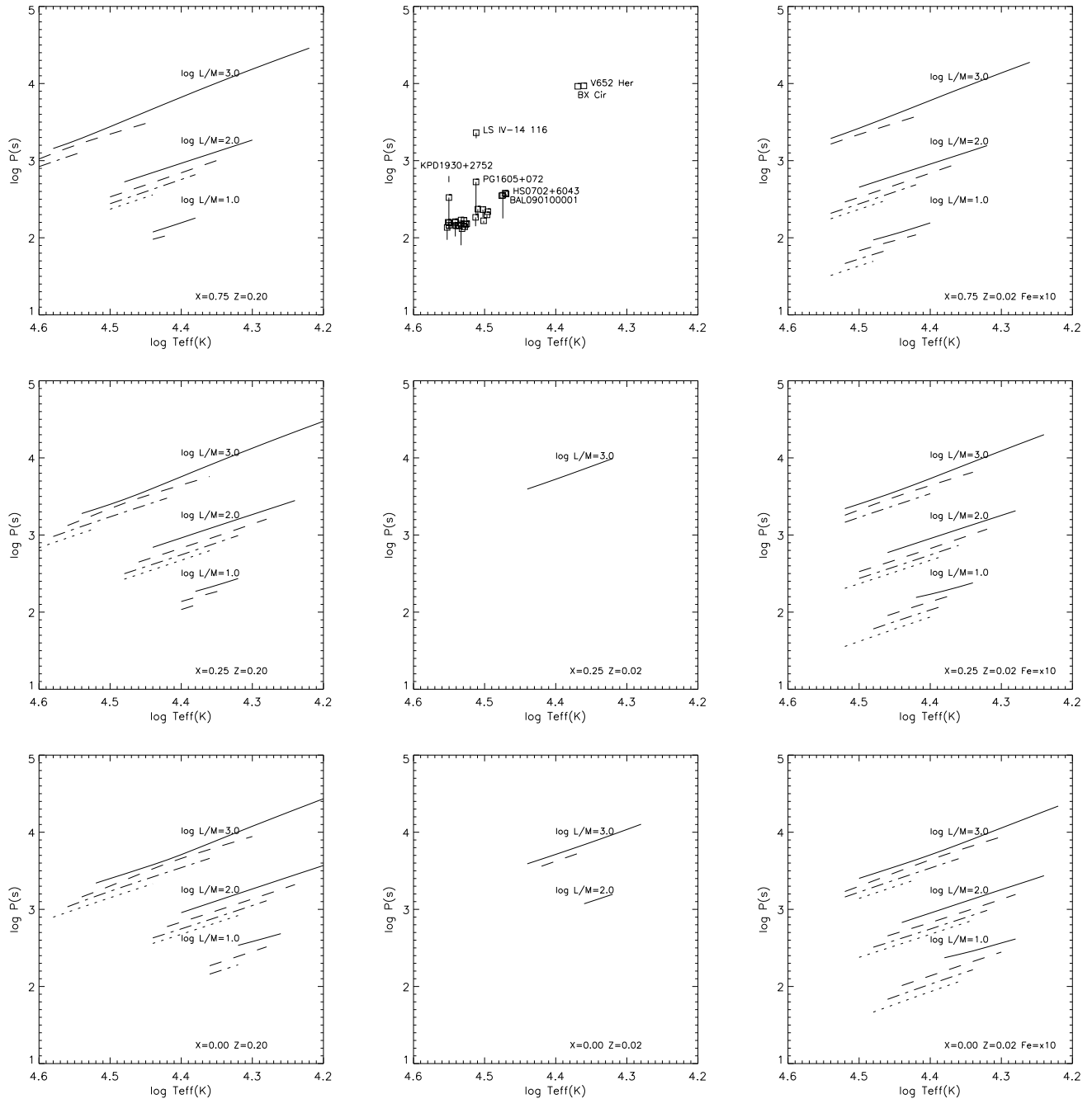


Figure 6. Periods of unstable modes due to Fe-bump instability for stars with $M = 0.50 M_{\odot}$ and $\log L/M = 1, 2$ and 3 . Each panel shows the fundamental (solid), first (dashed), second (dot-dashed) and third (dotted) harmonics. The middle column shows models with a standard metal content ($Z = 0.02$) and with X increasing upwards (there are no unstable modes for $X = 0.75, Z = 0.02$ at the L/M ratios shown). The left hand column shows models with enhanced $Z = 0.20$, the right hand column shows models with enhanced iron only ($f = 10$). Both columns show models with $X = 0.0, 0.25, 0.75$ increasing upwards. The loci of selected pulsating stars are shown in the centre - top panel; multi-periodic stars are shown by their longest period (square) and their range (line). The selection includes pulsating sdB stars and extreme helium stars.

although the precise periods of p-modes with spherical degree $l > 0$ will differ from the corresponding radial ($l = 0$) values.

Gravity modes propagate most strongly in the deep interior of the star. Consequently complete stellar models including both core and envelope are required. Following pre-

vious work (Fontaine et al. 2003) we have assumed that the PG1716 variables are extreme horizontal branch stars and have thus constructed series of “zero-age” horizontal-branch models having a helium-burning core with a mass of M_c and with a hydrogen-rich envelope with mass M_e ranging from 0.0003 to $0.0034 M_{\odot}$. We have considered two cases of M_c ;

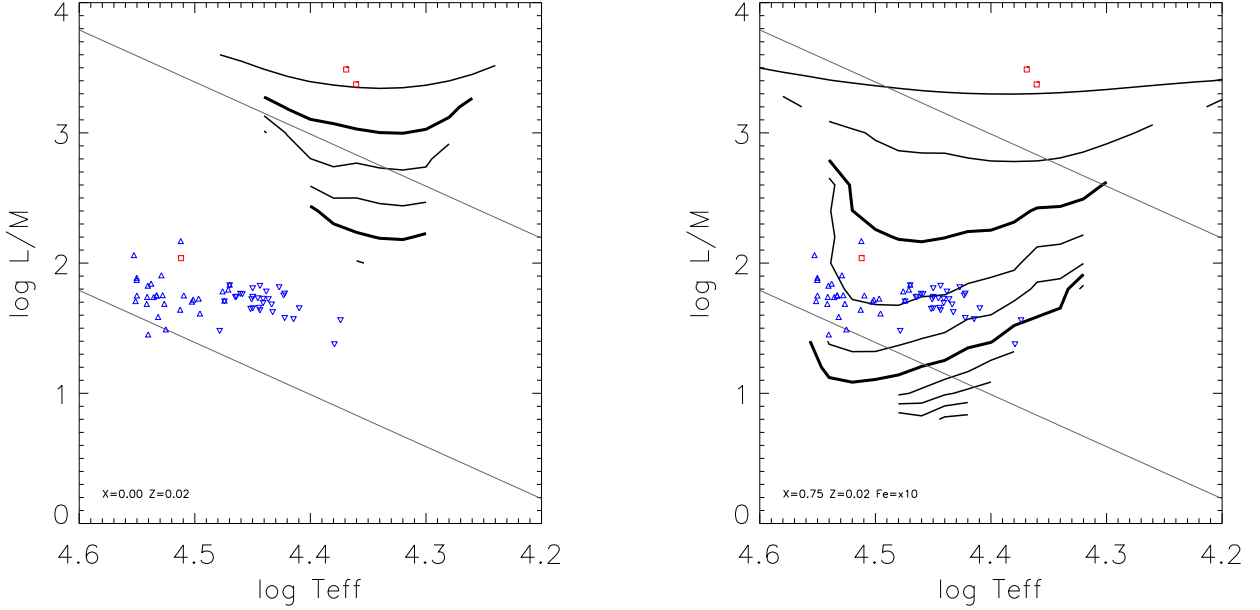


Figure 8. Contour plots representing minimum growth times for unstable modes in stars with $M = 0.50 M_{\odot}$ and for compositions representative of extreme helium stars (left) and EC14026 variables (right). Contours are separated by 1 dex, the bold lines representing $\log(-\omega_r/\omega_i) = 3$ and 6, with growth times decreasing toward higher L/M . Other features as in Fig. 1.

0.476 and $0.486 M_{\odot}$. The surface layers are characterized by mass fractions of hydrogen X and base metallicity Z_0 , with iron again augmented by a factor f . We have considered sequences with $X = 0.90, 0.75$ and 0.5 , with $Z_0 = 0.01$ and 0.02 , and with $f = 1, 10$ and 20 . The hydrogen abundance X_{tr} at the interface between a hydrogen-rich envelope and a helium core is assumed to be given as

$$X_{\text{tr}}(M_r) = 0.5X(1 + \sin \theta) \quad (5)$$

with

$$\theta \equiv \pi[(M_r - M_c)/\Delta M - 1], \quad (6)$$

where M_r is the mass coordinate within the transition layer, and ΔM , which is assumed to be $2 \times 10^{-4} M_{\odot}$, is the mass of the transition layer.

The high-temperature end of this sequence corresponds with the locus of the short-period EC14026 variables. PG1716 variables are to be found at lower temperatures, with $25\,000 \lesssim T_{\text{eff}}/\text{K} \lesssim 29\,000$.

We have carried out a stability analysis for each of these models testing the stability of *non-radial* p- and g-modes spherical degree $l = 1, \dots, 4$. The frequency range considered is $0.2 \leq \omega \leq 20$, where ω is the angular frequency of pulsation normalized by $\sqrt{GM/R^3}$ with G being the gravitational constant. The stability of non-radial modes is found to be insensitive to M_c . We show results for $M_c = 0.486 M_{\odot}$. To allow for the likelihood that most horizontal branch stars have evolved away from their zero-age structure, we will demonstrate later that their principal stability characteristics survive through to the end of core helium burning.

As anticipated, we find no unstable p-modes with $l > 0$, for any models with normal iron abundance ($f = 1$). Like the radial modes, these are only excited with significant iron

enhancements. Unexpectedly, we *do* find excited g-modes $l > 1$ in ZAHB stars with $Z = 0.02$ and no iron enhancement over a small interval $16\,000 < T_{\text{eff}}/\text{K} < 20\,000$, with $l = 2$ modes being excited in higher radial-orders and at lower T_{eff} than $l = 3$ and $l = 4$ modes (Fig. 9).

Some properties of an excited g-mode of $l = 2$ are shown in Fig. 10, where the solid line in the bottom panel is the radial displacement of pulsation divided by the distance from the center ξ_r/r , the dotted line is the work W , and the top panel shows the distribution of the kinetic energy of the mode. If a pulsation mode is excited (unstable), $W > 0$ at the surface. There is an excitation zone ($dW/dr > 0$) in a temperature range of $5.1 \lesssim \log T \lesssim 5.4$ due to the Fe-opacity bump and a damping zone ($dW/dr < 0$) just below. This g-mode is marginally unstable because the driving effect is not very strong with no enhancement of iron abundance. In such a case, a reflection of the wave at the interface between the core and hydrogen-rich envelope plays an important rôle. Fig. 10 shows that the kinetic energy and the amplitude of the mode suddenly decrease towards the center at $\log T \sim 7.25$, where the hydrogen abundance changes steeply, indicating a partial reflection of the mode to occur there. A sudden change in the mean molecular weight at the interface requires a sudden change in the gas density, which reflects g-modes partially. The reflection reduces the amplitude in the core and hence reduces radiative damping there. The strength of the reflection depends on the phase of the spatial oscillation at the interface, and hence only some of the g-modes are excited in the optimal period range for the Fe-bump mechanism.

One model for which g-modes are excited on the ZAHB was evolved through its complete horizontal-branch evo-

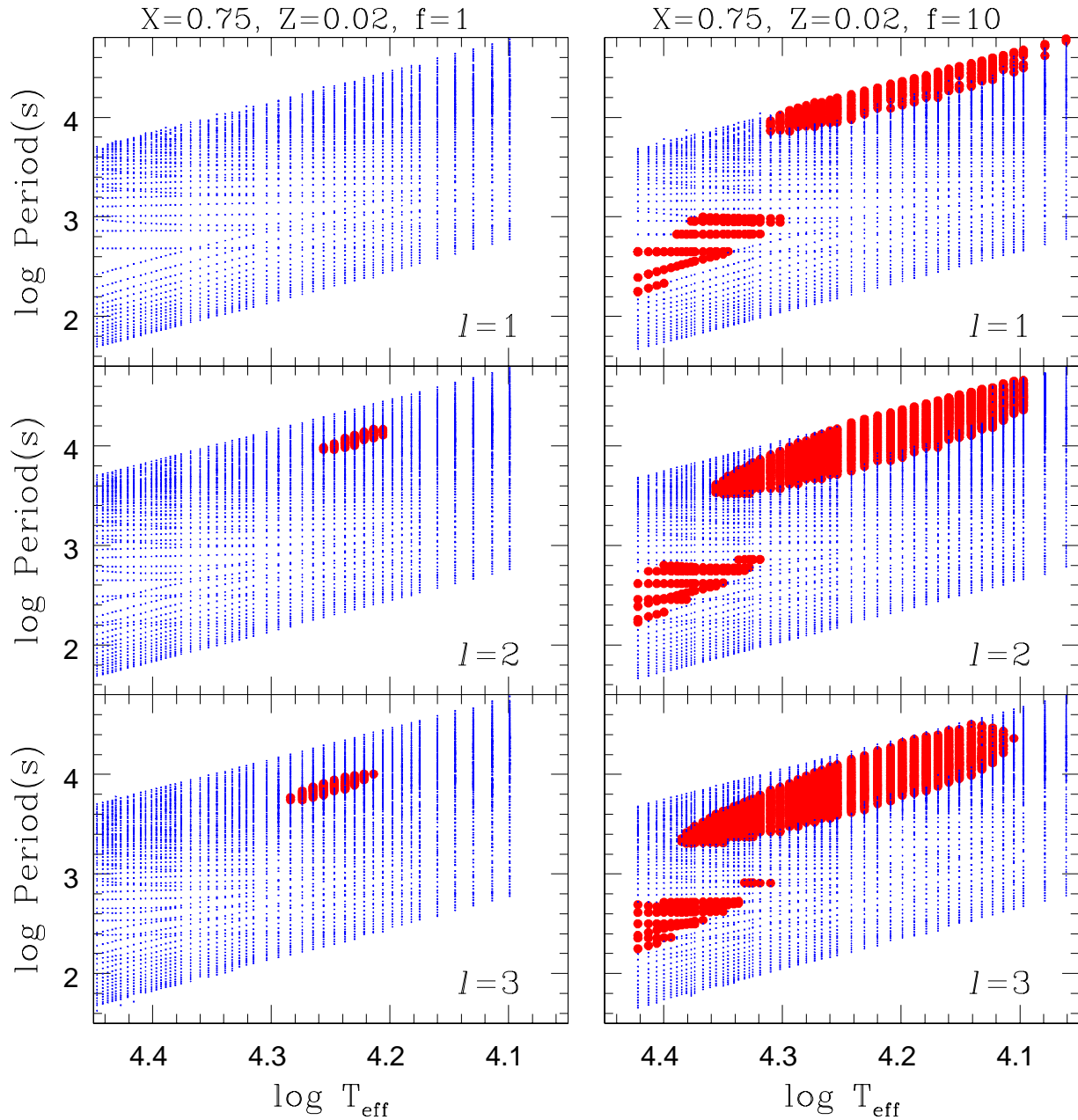


Figure 9. Periods of modes due to Fe-bump instability for ZAHB stars with $M_c = 0.486 M_\odot$, $X = 0.75$ and $Z_0 = 0.02$, and M_{rme} is increasing from right to left. The left hand column shows models with no additional iron enhancement ($f = 1$), the right hand column shows models with iron increased by a factor $f = 10$. Stable modes are marked as (blue) dots, unstable modes are marked as filled (red) circles. The chemical mixture with $f = 1$ corresponds to that in the first column, second row of Figs. 4 and 5, while that with $f = 10$ corresponds to that in the third column, second row of Figs. 4 and 5.

lution. The g-modes continue to be excited throughout HB evolution, primarily because, with no hydrogen-burning shell, the basic structure of the envelope and the characteristics of the core-shell reflection surface are not altered.

The above result indicates that g-mode pulsations can be driven in certain blue horizontal branch stars irrespective of whether chemical stratification enhances the iron-

abundance in the driving zone. This conjecture will require observational verification, which will constrain theoretical models for the blue horizontal branch stars. Moreover, it implies that g-modes in these cooler stars are more likely to be excited with modest iron enhancements than the p-modes. The growth times for the ZAHB models are relatively long

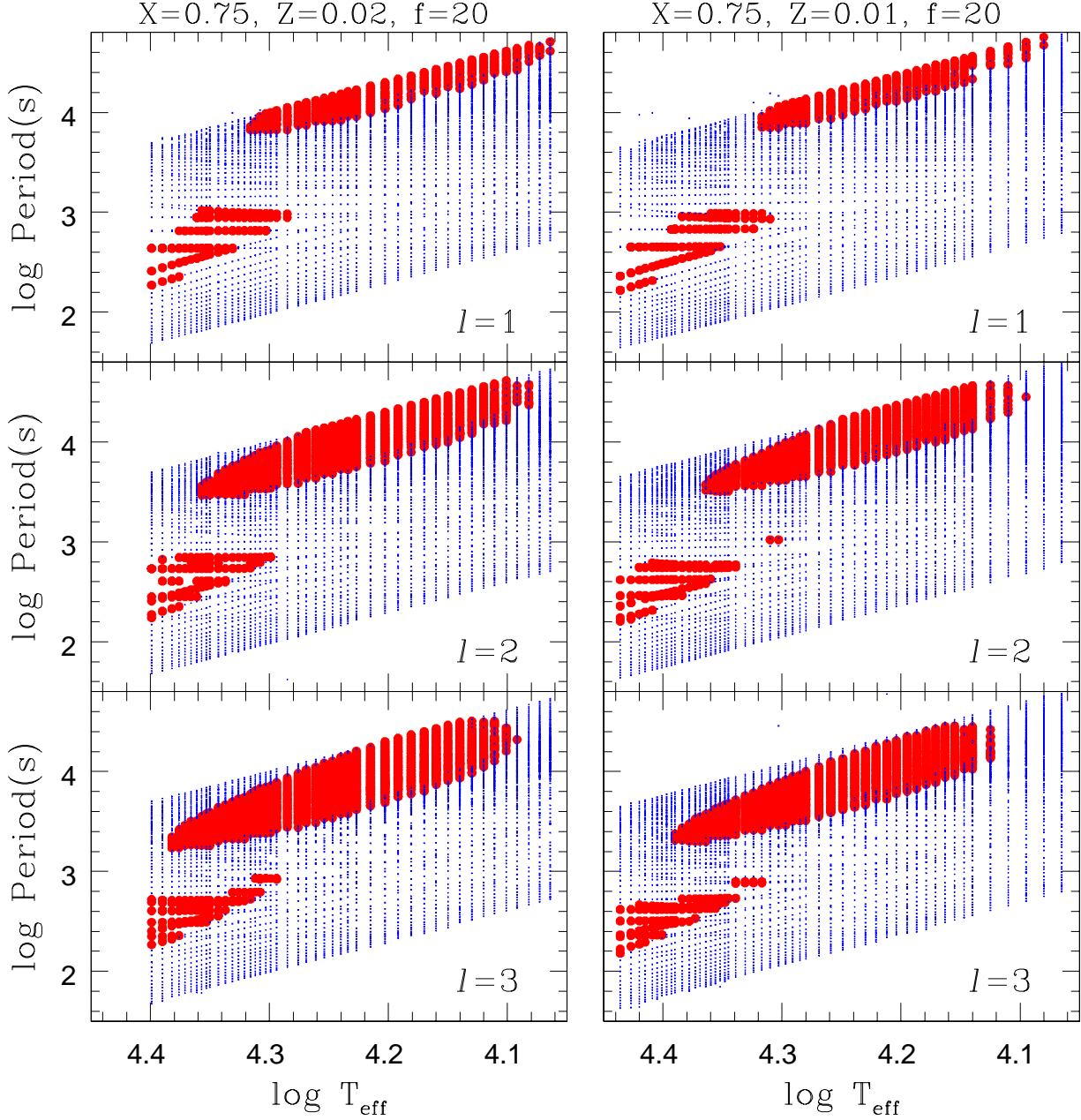


Figure 11. As Fig. 9, for models with $M_c = 0.486 M_\odot$, $X = 0.75$ and iron enhancement $f = 20$, but for $Z = 0.02$ (left) and 0.01 (right), demonstrating the shift of the g-mode blue edge with metallicity Z .

(~ 100 y, Fig. 10), but are reduced by factors of ~ 10 during HB evolution.

However, in general, unstable modes (both p- and g-) are only recovered with a significant enhancement of iron. Indeed, with $f \sim 10$, we always find unstable modes of either p- or g-type down to $T_{\text{eff}} \sim 13000\text{K}$ (Fig. 9). In these models, the reflection at the core boundary is not important in the excitation of g-modes, and most modes are excited in an optimal range of periods. The growth times for these modes are $\sim 1 - 10$ y. The locus of the p-mode instability

follows that of the radial modes as a function of X , Z and f .

In our models, with $f \geq 10$, the high temperature limit of the unstable g-modes always overlaps the low-temperature limit of the unstable p-modes of the same spherical degree. While this overlap is marginal for $l = 1$ modes, it increases substantially with l . This result has an important corollary which states that if a star has an effective temperature such that it is in the p- and g-mode instability overlap (p/g overlap) and if p-mode oscillations

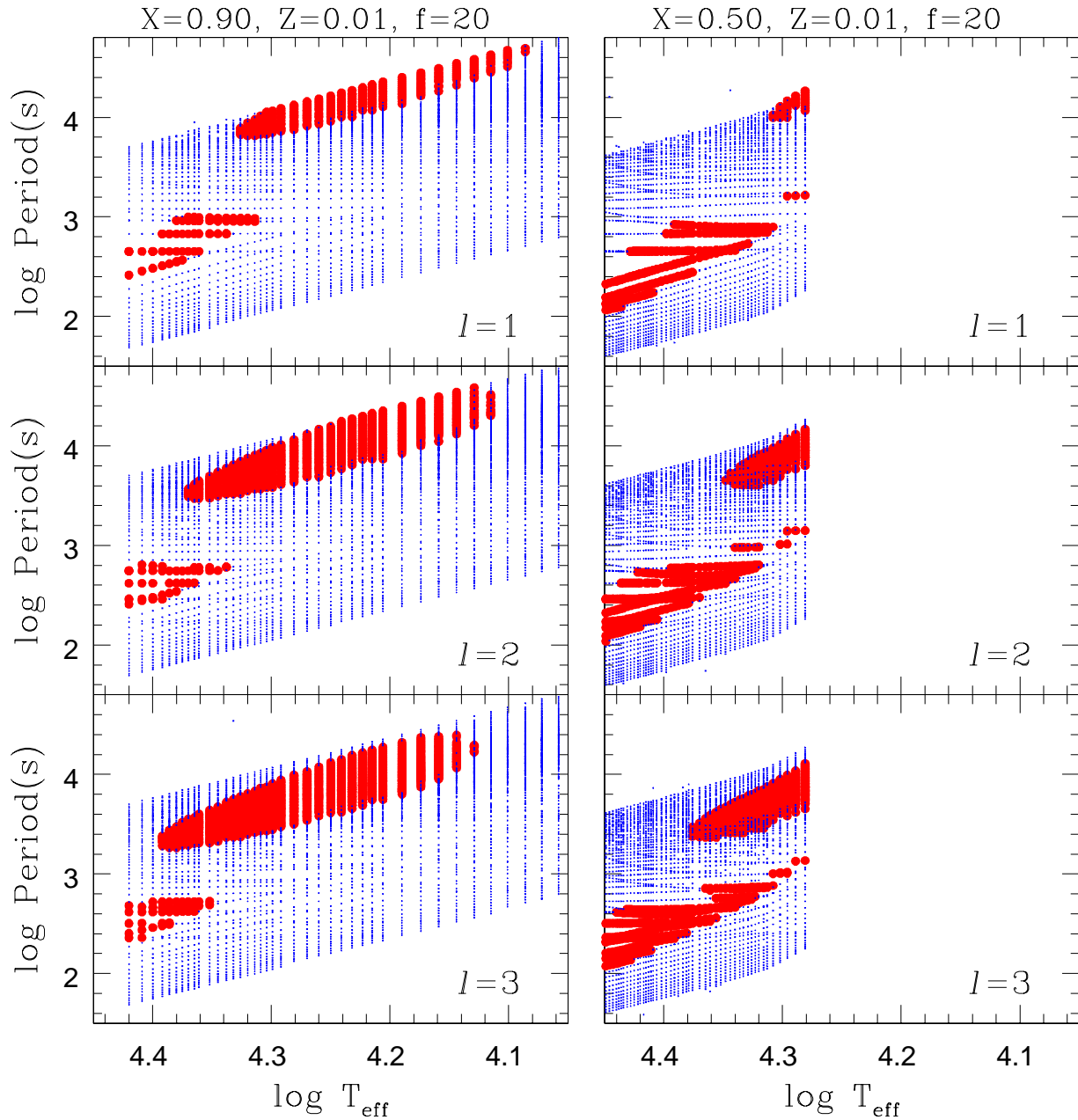


Figure 12. As Fig. 9, for models with $M_c = 0.486 M_\odot$, $Z = 0.02$ and iron enhancement $f = 20$, but for $X = 0.90$ (left) and 0.50 (right), demonstrating the shift of the g-mode blue edge with hydrogen fraction X .

are observed, *i.e.* it is an EC14026 variable, then the iron enhancement necessary to drive the p-modes will also be sufficient to drive the g-modes, *i.e.* it is also likely to be a PG1716 variable.

This is true regardless of the fact that we have used a global iron enhancement rather than a stratified model. The reason is that the driving for both p- and g-modes comes from the same part of the star, so that for a star of the right effective temperature, it may actually be impossible to have p-mode instability without g-mode instability. In-

deed, the stars Balloon 090100001 and HS 0702+6043 lie on the boundary between the observed EC14026 and PG1716 variables and exhibit both types of pulsational behaviour (Schuh et al. 2006; Oreiro et al. 2005).

However, there is a problem. The high temperature limit of the unstable g-modes occurs around $T_{\text{eff}} \sim 20000$ K for $l = 1$ modes, increasing to ~ 25000 K for $l = 4$. The observed high temperature limit for PG1716 variables is ~ 29000 K and it is unlikely that $l > 2$.

We have investigated g-mode stability for ZAHB mod-

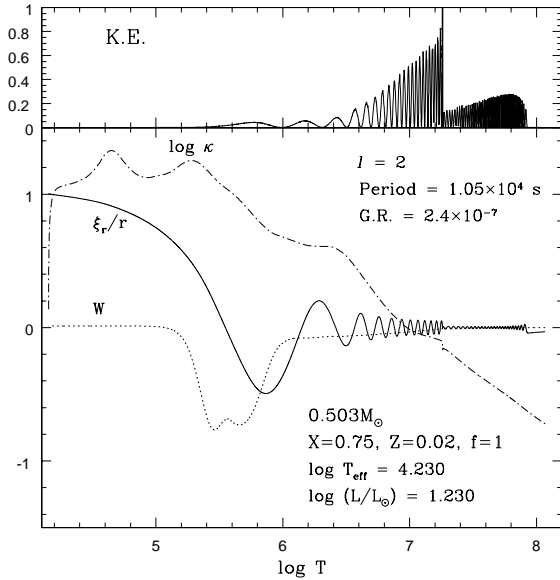


Figure 10. The bottom panel shows the radial displacement ξ_r and work W of an unstable high-order g-mode of $l = 2$, and opacity κ as a function of the temperature. In a driving (damping) zone, $dW/dr > 0$ (< 0), and the mode is unstable if $W > 0$ at the surface. The top panel shows the distribution of the kinetic energy of the mode. A sudden change in the kinetic energy and in the amplitude of the spatial oscillation at $\log T \approx 7.25$, where the hydrogen abundance changes steeply. The convective core, where the g-modes are (spatially) evanescent, extends to $\log T = 7.934$. G.R. is the growth rate $-\omega_i/\omega_r$.

els having a range of chemical composition. Figs. 11 and 12 demonstrate the effects of varying the overall metallicity Z or the overall hydrogen concentration X whilst maintaining a high iron concentration ($f = 10$). Increasing X (equivalent to reducing the helium fraction) has the effect of a modest increase in the effective temperature of the g-mode blue edge. Similarly, reducing Z while conserving the iron abundance (Fig. 11) shifts the blue edge of g-modes blueward a little. These effects can be understood from equation (4). However, in neither case is a substantial change in the envelope composition capable of shifting the g-mode blue-edge to its observed location.

Figs. 9 to 12 exclude results for $l = 4$. The $l = 4$ blue edge is always bluer than the $l = 3$ blue edge by ~ 0.01 dex. In addition to the lower likelihood of observing $l = 4$ modes, this is again insufficient to account for the observed blue edge.

These results closely mirror those obtained previously (Fontaine et al. 2003), where radiative levitation provides the necessary enhancement in the iron abundance in the driving region. These authors found g-mode instability with $l = 3, 4$ at effective temperatures up to 24000 K ($\log T_{\text{eff}} \leq 4.38$), or with $l \leq 8$ up to $\log T_{\text{eff}} \leq 4.43$, still too cool to account for the observed blue edge. The main difference is that our models show unstable g-modes at $l = 1$ and 2 where those of Fontaine et al. did not. One reason may be that our model envelopes have a homogeneous chemical

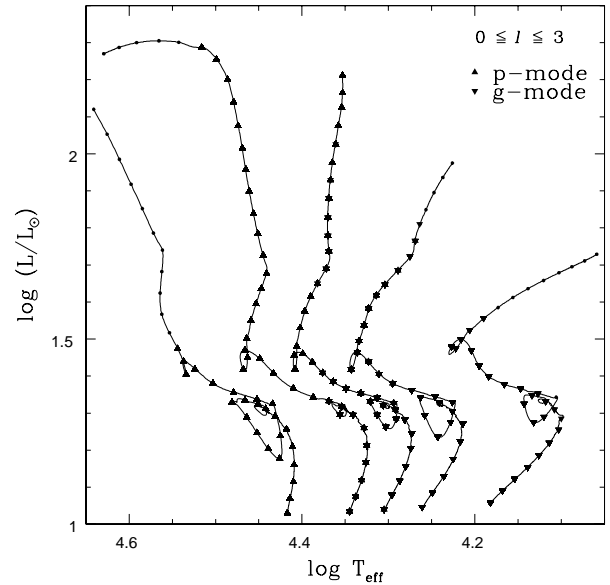


Figure 13. Evolution tracks for horizontal branch stars with $M_c = 0.476 M_\odot$, $X = 0.75$, $Z_0 = 0.02$ and enhanced iron abundance $f = 10$. Total masses are $M = 0.4763, 0.478, 0.480, 0.483$ and $0.490 M_\odot$. Models having either unstable p- or g-modes with $l < 4$ are indicated by (\blacktriangle) and (\blacktriangledown), respectively. Small dots indicate models in which neither is excited. Note that models having both unstable p- and g-modes appear as “stars”.

composition with an artificial iron enhancement, whereas the earlier models have a stratified composition with iron enhanced in critical layers by a well-understood mechanism.

We have found that the effective temperature at the blue edge of g-modes hardly changes when the degree of iron enrichment increases as long as $f \geq 10$. This indicates that to have a blue edge of g-modes consistent with the observation, we have to change something in the structure of models.

Evolved horizontal-branch stars

One solution to the blue-edge question might be to consider the evolution of these stars. We have computed the evolution of iron-enriched extended-horizontal branch models with $X = 0.75$, $Z_0 = 0.02$, $f = 10$ and $M_c = 0.476 M_\odot$ through the completion of core helium-burning and beyond (Fig. 13). Note the “breathing pulses” (small loops in the HR diagram) towards the end of core helium-burning. These are encountered in our models with artificially high iron abundances. They are due to the increased core opacity and are not significant in models with a normal core composition. Semiconvection is included following the description by Spruit (1992).

We have carried out a stability analysis for selected models along each evolutionary sequence. Fig. 13 shows those models where either p-modes and/or g-modes are unstable for $l < 4$. Comparing the instability temperature range of zero-age models for the same composition,

we see that stability of p-modes are hardly affected by the evolutionary change of the stellar structure, while g-modes tend to be damped in evolved models in which the central part is radiative. There is a clear overlap region $4.30 < \log T_{\text{eff}}/\text{K} < 4.38$, where both p- and g-modes are unstable. This extends upwards in luminosity to include some post-horizontal-branch stars; it does not extend blue-wards.

The Brunt-Väisälä frequency becomes extremely large in the evolved non-degenerate radiative core. This makes the wavelength of a g-mode very short, which in turn enhances the radiative damping and stabilizes the mode. Still some g-modes are excited even in evolved models with a radiative core. For these models a partial reflection at the bottom of the helium-rich envelope reduces the amplitude and hence radiative damping in the core. Since only few g-modes are excited and the evolutionary speed is fast, these g-modes are not very important observationally.

4 CONCLUSION

Our original goals were to understand oscillations observed in the helium-rich subdwarf LSIV-14°116, and in the PG1716 variables. We therefore carried out a broad review of Fe-bump driven pulsational instability in low-mass stars¹.

By first considering radial modes, we have demonstrated the essential rôle of chemical composition such that instability increases with the contrast between the iron-bump opacity and other opacity sources. This increased contrast may be achieved either by increasing the iron abundance, confirming earlier work by Charpinet et al. (2001) or by reducing the hydrogen abundance (Jeffery & Saio 1998). At least one of these is necessary to excite oscillations in all of the *low-mass* Fe-bump pulsators discovered to date.

We have further demonstrated that the blue-edge for radial instability is affected by the mean molecular weight in the stellar envelope, so that increasing the iron abundance alone provides a bluer instability region than increasing the iron abundance in concert with all elements heavier than helium. The former is required to explain the locus of the EC14026 instability region, making the general assumption that the properties of non-radial p-modes are closely linked to the corresponding radial mode of the same radial order.

Furthermore, the blue-edge also depends on the radial order of the oscillations, so that higher-order modes may be found in hotter stars. By comparing theoretical and observed periods for EC14026 stars, we have shown that low-order or fundamental mode radial oscillations are only likely to be seen in the coolest EC14026 stars and that the hottest stars must oscillate in higher-order modes.

However, we have been unable to explain the oscillations in the helium-rich star LSIV-14°116; the observed periods are simply too long compared with the L/M ratio obtained from spectroscopy. A lower surface gravity would definitely help.

Considering non-radial pulsations, we have focused on g-mode instability and in particular on instability in modes

with spherical degree $l < 4$. We have discovered a small g-mode instability island on the blue horizontal branch which does not require iron enhancement or hydrogen depletion. However, since it requires $Z = 0.02$ and a partial reflection of the wave at the interface between the hydrogen-rich envelope and the helium core, it will take some observational effort to verify whether there are any real pulsating horizontal-branch stars which correspond with these models. Effective temperatures are expected to be between 16 000 and 20 000 K, and pulsation periods between 1 and 4 hours.

With a factor of 10 enhancement of iron on a background metallicity $Z = 0.02$, a large instability region develops, even for $l = 1$, which extends from $< 13\,000$ to $\sim 24\,000$ K ($l = 3$). With such iron enhancement there is always an overlap between p- and g-mode instability regions so that stars near the boundary would be expected to exhibit both modes simultaneously. Depleting the envelope hydrogen abundance tends to shift both the g-mode blue edge and the radial/p-mode red edge to lower temperatures.

Many of these results have been demonstrated individually (Saio 1993; Jeffery & Saio 1998; Charpinet et al. 1996; Fontaine et al. 2003); this investigation has placed them in a more general context, as well as delivering some new results. Of these, the rôle that mean molecular weight plays in determining the instability boundaries for radial and p-mode oscillations has implications for understanding the oscillations in EC14026 variables. We have made no effort to justify the adopted abundances on physical grounds, we have simply sought parametric solutions which satisfy the observations. Radiative levitation (Chayer, Fontaine & Wesemael 1995) is known to operate in extreme horizontal-branch stars and provides a natural explanation for the required iron enhancements. The fact that it operates selectively accords well with our deduction that only iron should be enhanced.

Our discovery that g-mode oscillations may be excited in blue horizontal branch stars with envelopes of “normal” composition has two-fold consequences. In addition to the observational question already posed, it may be less hard to excite g-mode pulsations in PG1716 stars than hitherto supposed; maybe we don’t have to work so hard to find the necessary chemical structure in the stellar envelope as we do in the case of EC14026 variables.

Nonetheless, we have been unable to resolve the problem of why the observed boundary between the EC14026 and PG1716 stars occurs at $\sim 29\,000$ K. The theoretical p-mode/g-mode boundary remains persistently at $\sim 24\,000$ K over a wide range of envelope compositions. It is possible that a sharp discontinuity in composition immediately below the iron bump could help; this and other experiments with stratified envelopes remain to be investigated.

ACKNOWLEDGMENT

Travel support for this collaborative project was provided through PPARC grant PPA/G/S/2002/00546.

REFERENCES

- Ahmad A., Jeffery C.S., 2003, A&A 402, 335
- Ahmad A., Jeffery C.S., 2005, A&A 437, L51

¹ Oscillations in main-sequence stars were deliberately excluded from our study.

- Billères M., Fontaine G., Brassard P., Charpinet S., Liebert J., Saffer R.A., Vauclair G., 1997, *ApJ* 487, L81
- Billères, M., Fontaine, G., Brassard, P., Charpinet, S., Liebert, J., Saffer, R.A., 2000, *ApJ* 530, 441
- Brassard, P., Fontaine, G., Billères, et al., 2001, *ApJ* 563, 1013
- Charpinet S., Fontaine G., Brassard P., Dorman B., 1996, *ApJ* 471, L103.
- Charpinet S., Fontaine G., Brassard P., Chayer P., Rogers F.J., Iglesias C.A., Dorman B., 1997, *ApJ* 483, L123.
- Charpinet S., Fontaine G., Brassard P., 2001, *PASP* 113, 775
- Charpinet S., Fontaine G., Brassard P., Green E.M., Chayer P., 2005a, *A&A* 437, 575
- Charpinet S., Fontaine G., Brassard P., Billères M., Green E.M., Chayer P., 2005b, *A&A* 443, 251
- Chayer P., Fontaine G., Wesemael, F., 1995, *ApJS* 99, 189
- Cox J.P., 1980, *Theory of Stellar Pulsation*, Princeton University Press; Princeton
- Dziembowski W.A., Pamiatnykh A.A., 1993, *MNRAS* 262, 204
- Fontaine G., Brassard P., Charpinet S., Green E.M., Chayer P., Billères M., Randall S.K., 2003, *ApJ* 597, 518
- Gautschy A., Glatzel W., 1990, *MNRAS* 245, 154
- Green E.M., Fontaine, G., Reed M., et al., 2003, *ApJ* 583, 31.
- Grevesse N., Noels A., 1993, in *Origin and Evolution of the Elements*, p.15, ed. N.Pratzo, E. Vangioni-Flam, & M. Casse, Cambridge University Press
- Iglesias C.A., Rogers F.J., 1996, *ApJ* 464, 943
- Jeffery C.S., Harrison, P.M., 1997, *A&A* 323, 393
- Jeffery C.S., Hill, P.W., 1996, *Observatory* 116, 156
- Jeffery C.S., Saio H., 1998, *MNRAS* 308, 221
- Jeffery, C.S., Woolf, V.M., Pollacco, D.M., 2001, *A&A* 376, 497
- Kanbur, S.M., Simon, N.R., 1994, *ApJ* 420, 880
- Kilkenny D., Koen C., 1995, *MNRAS* 275, 327
- Kilkenny D., Koen C., O'Donoghue D., & Stobie R.S., 1997, *MNRAS* 285, 640
- Michaud G., Bergeron P., Wesemael F., Heber U., 1989, *ApJ* 338, 417
- Moskalik, P., Buchler, J.R., Marom, A., 1992, *ApJ* 385, 685
- Oreiro R., Pérez Hernández F., Ulla A., Garrido R., Østensen R., MacDonald J., 2005, *A&A* 438, 257
- Rogers F.J., Iglesias C.A. 1992, *ApJS* 79, 507
- Saio H., 1993. *MNRAS* 260, 465
- Saio H., 1994. *CCP7 Newsletter* 21, 50, ed. C.S.Jeffery, Univ. of St Andrews
- Saio H., 1995. *MNRAS* 277, 1393
- Saio H., Baker N.H., Gautschy A., 1998, *MNRAS* 294, 622
- Spruit, H.C., 1992, *A&A* 253, 131
- Schuh S., Huber J., Dreizler S., Heber U., O'Toole S.J., Green E.M., Fontaine G., 2006, *A&A* 445, L31
- The Opacity Project Team, 1995, *The Opacity Project*, Vol. 1, IoP, Bristol
- Woolf, V.M., Jeffery, C.S., 2002, *A&A* 395, 535